Investigating the mechanism of action of the anti-aging ability of Geraniin nano-phytosome (GNP)

Asly Poh-Tze Goh[1], Uma Devi Palanisamy [1], **Usha Sundralingam[2*]**

[1]Jeffrey Cheah School of Medicine and Health Sciences, Monash University Malaysia, Jalan Lagoon Selatan, Bandar Sunway 47500, Selangor, Malaysia.

[2]School of Pharmacy, Monash University Malaysia, Jalan Lagoon Selatan, Bandar Sunway 47500, Selangor, Malaysia.

[*]Corresponding author e-mail: usha.sundralingam@monash.edu

Abstract

In the dynamic realm of cosmetics, geraniin, a potent antioxidant derived from fruit waste, emerges as a sustainable solution for anti-aging. Overcoming challenges in intestinal absorption, this study explores a topical application of geraniin, focusing on its skin anti-aging mechanisms and developing a novel GNP. Geraniin extracted from *Nephelium lappaceum* (Rambutan) rind, and its skin anti-aging effects were assessed through various mechanistic assays. The GNP formulation was developed using purified geraniin, soy phosphatidylcholine, squalene, and various edge activators. The optimized GNP was characterized for its physical-chemical properties. An *in vitro* permeation study on synthetic membrane (Strat-M®) using Franz diffusion cell to determine the permeability of GNP was conducted. Geraniin strongly inhibited collagenase, moderately inhibited elastase, and effectively blocked AGE formation, suggesting its potential in preventing skin aging. Characterization of the optimized formulation revealed an entrapment efficiency of 67.61 ± 2.06%, a particle size of 95.60 ± 0.46 nm, and a polydispersity index of 0.167 ± 0.014, with Tween 80 providing the most stable formulation. Permeation studies revealed accumulation of geraniin within the membrane, confirming its suitability as a topical application. This study highlights geraniin's anti-aging potential and the creation of a stable nano-phytosome, making it a suitable eco-friendly skincare formulation.

Keywords: Anti-aging; nano-phystosome; geraniin; elastase; AGE; collagenase

1. Introduction.

Skin, as the body's most exposed organ, is not only a complex barrier but also a visible indicator of aging [1]. The condition of one's skin reflects overall health and can even predict life expectancy [2]. Aging, an unavoidable process, significantly affects human skin, manifesting as either chronological aging or photoaging [3]. Over time, skin is impacted by both external [4] and internal factors [5], such as light exposure, pollution, and disease, all of which contribute to aging. Historically, several theories have been proposed to explain the causes and mechanisms of skin aging, including oxidative stress theory, skin photoaging theory, inflammation theory, and metabolism theory [6-8]. Skin aging involves the degradation of the extracellular matrix (ECM), primarily composed of collagen and elastin, which are crucial for skin elasticity and structural integrity [9]. The decline in these components leads to visible signs of aging, such as wrinkles. Reactive oxygen species (ROS), exacerbated by UV radiation, contribute to oxidative stress and skin aging through cellular damage [10]. Thus, given the significant role of oxidative stress in skin aging, most anti-aging strategies and products focus on enhancing antioxidant defenses. In the past, effective anti-aging products were primarily derived from chemically extracted plant extracts and natural small molecule compounds.

Natural products have long been pivotal in treating various health challenges, a tradition that persists due to increasing public health awareness and demand for herbal plants [11, 12]. The World Health Organisation (WHO) notes that 75% of the global population has relied on herbal plants for basic healthcare over the past three decades [12]. Recently, there has been a surge of interest in using natural plant extracts in the cosmetic industry, as they provide a preferable alternative to synthetic agents by offering antioxidant, antimicrobial, and anti-aging benefits [13]. Mechanistic studies have shown that these natural products exert their anti-aging effects

by inhibiting enzymes such as tyrosinase, which is involved in melanin production and hyperpigmentation; hyaluronidase, which degrades hyaluronic acid and contributes to skin aging; advanced glycation end-products (AGEs), which accelerate aging through cross-linking of collagen fibers; and collagenase and elastase, which breaks down collagen, leading to loss of skin firmness and elasticity [14].

Among these natural products, several stand out for their remarkable anti-aging properties. Aloe vera, for example, enhances collagen and elastin synthesis, significantly improving skin elasticity and reducing the appearance of wrinkles [15]. Honey, rich in phenolic compounds, offers potent antioxidant activities, effectively protecting the skin from oxidative stress and preventing premature aging [16]. Pomegranate peel contains a wealth of bioactive compounds that not only reduces age spots and wrinkles but also promotes the regeneration of skin cells, leading to a more youthful and vibrant complexion [17, 18].

Geraniin, an ellagitannin found in various fruits, stands out for its strong antioxidant properties, which contribute significantly to its anti-aging potential [19, 20]. A recent *in vitro* study demonstrated the antioxidant potential of Rambutan (*Nephelium lappaceum L*.) rind extracts and geraniin on human epidermal keratinocytes [21]. However, despite its numerous benefits, geraniin's high molecular weight poses a challenge for skin penetration, limiting its efficacy [22]. To overcome this limitation, advancements in nanotechnology, particularly the use of nano-phytosomes, offer a promising solution. Nano-phytosomes can enhance the delivery and efficacy of geraniin by improving its bioavailability and bioactivity, thus making it more effective in anti-aging applications [23].

The development of geraniin nano-phytosomes (GNP), derived from the waste rind of rambutan (*Nephelium lappaceum L.*), represents a significant stride in sustainable practices

and aligns with forward-thinking government policies. Malaysia, a leading producer of rambutans, faces considerable challenges with agricultural waste from the canning industry. By transforming rambutan rind into high-value products, this innovative approach not only addresses waste management issues but also promotes economic and environmental sustainability. This initiative supports Malaysia's national development plan, particularly the Entry Point Project 7 (EPP 7) and the National Key Economic Area (NKEA) in the Agriculture sector, showcasing a powerful synergy between scientific advancement and sustainable economic growth [24]. Thus, this study aims to uncover the potent skin anti-aging properties of geraniin and the novel GNP formulation, ultimately delving into their mechanisms of action.

2 Materials and Methods.

2.1 Materials

Purified geraniin from *Nephelium lappaceum* rind (purity of 99.4%), acetonitrile (ACN), ethanol, dichloromethane, formic acid, lecithin L-alpha-phosphatidylcholine (Lipoid EPC), sodium di-hydrogen phosphate (NaH_2PO_4), sodium hydroxide (NaOH) pellets, sodium chloride (NaCl) and hydrochloric acid (HCl) were obtained from Sigma-Aldrich (Missouri, USA). Acetone, tetrahydrofuran and n- octanol were purchased from Merck (Darmstadt, Germany). Chloroform and ethyl acetate were obtained from Mallinckrodt Chemicals (New Jersey, USA). Phosphate buffer saline (PBS) was purchased from Gibco-Invitrogen (California, USA). Soy phosphatidylcholine (SPC) was purchased from Avanti Polar Lipids Inc (Alabama, USA). STGaia™ (Squalene) was gifted by PhytoGaia Sdn. Bhd. (Malaysia). All other chemicals and reagents used in this study were of analytical grade.

2.2 Methods

2.2.1 Skin aging inhibitory action assay

2.2.1.1 Advanced glycation end products (AGE) formation inhibitory activity (BSA-MGO)

The inhibitory activity on AGE formation was assessed using bovine serum albumin-methylglyoxal (BSA-MGO) model systems as described previously [25]. BSA (2 mg/mL) and MGO (400 mg/mL) were dissolved separately in phosphate buffer (pH 7.4). Geraniin, crude extract, squalene and ellagic acid (1 mg/mL) was mixed with 1 mL of BSA and 1 mL of MGO solution in a 5 mL Eppendorf tube, respectively. A blank and solvent control was prepared with 1 mL of phosphate buffer or 5% DMSO, 1 mL of BSA solution and 1 mL of MGO solution. A positive control was prepared by mixing 1 mL of aminoguanidine solution (1M) with 1 mL of BSA solution and 1 mL of MGO solution. The tested solution also included 0.01% (w/v) of sodium azide (NaN_3) to inhibit microbial growth. The samples were incubated in the dark at 37°C for seven days. The fluorescence was measured after incubation at excitation and emission wavelengths of 340 nm and 420 nm using Tecan Infinite M200 Microplate Reader. Triplicate samples were run for each sample and the percentage of inhibition was calculated using **equation 1**: (FI: fluorescence intensity)

$$\text{Inhibition (\%)} = \frac{1 - (\text{FI of sample})}{(\text{FI of blank})} x\ 100 \qquad \textbf{(Equation 1)}$$

2.2.1.2 Collagenase inhibitory activity assay

The collagenase inhibition activities of geraniin, crude extract, squalene and ellagic acid were evaluated using EnzChek® Gelatinase/Collagenase (E-12055) [26]. The protocol was followed according to the manufacturer's instructions with some modifications.100µL of Clostridium

collagenase (0.2 units/L) was added to 80 µL of sample (1 mg/mL) or 1,10-phenanthroline (0.5 mM) as positive control and incubated in the dark for 10 mins at 37°C. The blank was prepared using the reaction buffer as a control. After pre-incubation, 20 µL of DQ gelatin (1 mg/mL) was added to the reaction well. The plate was further incubated for 15 mins at 37°C. The fluorescence was measured at excitation and emission wavelengths of 495 nm and 515 nm using Tecan Infinite M200 Microplate Reader. Triplicate samples were run for each sample and the percentage of inhibition was calculated using **equation 1**.

2.2.1.3 Elastase inhibitory assay

The elastase inhibition activities of geraniin, crude extract, squalene and ellagic acid were assayed using EnzChek® Elastase Assay kit (E-12056) as previously described [27]. Porcine pancreatic elastase (100 µL; 0.5 units/mL) was mixed with 50 µL of sample (1 mg/mL) in a 96-well microplate and incubated at 25°C for 30 mins in the dark. DMSO (50 µL) and elastase inhibitor (N-Methoxysuccinyl-Ala-Ala-Pro-Val-chloromethyl ketone (MAAPV), 50 µL of 0.4 mM) was used as the control (no inhibitor) and positive control, respectively. The blank contained distilled water (50 µL) and 1X reaction buffer solution (100µL). After pre-incubation for 30 mins, 50 µL of the elastin working solution (100 µL) was added to each well and incubated at 25°C in the dark for 2 hours. The fluorescence intensity of the sample in each well was measured by a fluorescence microplate reader (Tecan Infinite M200 Microplate Reader) at an excitation wavelength of 485 nm and an emission wavelength of 520 nm. Triplicate samples were run for each sample and the percentage of inhibition was calculated using **equation 1**.

2.2.2 Preparation of Geraniin (GE) nano-phytosome (GNP)

The geraniin nano-phytosome (GNP) was prepared using a thin layer hydration method with various edge activators (Tween 80, Span 80, and sodium cholate hydrate) and solvents (absolute ethanol and dichloromethane) during preliminary studies. Consequently, the

formulation with Tween 80 was selected for further study, as detailed in **TABLE I**. Squalene was included as a preservative in the formulations. A concentration of 0.1% (w/v) geraniin was chosen for the formulation based on initial efficacy studies, which demonstrated that this dosage was well below the toxicity thresholds observed for geraniin [28]. The concentration of compositions in **TABLE I** was finalized following a detailed preliminary study. The resultant GNP was evaluated for its physical appearance, yield, entrapment efficiency, and permeability studies. Four sample groups were tested for physicochemical characterization (**TABLE II**).

Initially, all ingredients were dissolved in absolute ethanol within a round-bottom flask and mixed thoroughly for 30 mins. The mixture was then subjected to a rotary evaporator with the following conditions: water bath temperature set at 40°C, pump pressure at 150 hPa, rotary speed at 300 rpm, and refrigerator temperature at 4°C. This process was continued until a thin dry film formed on the wall of the flask.

TABLE I: Composition of formulations prepared.

Materials	**Concentration (% w/v)**					
	E1	E2	E3	E4	E5	E6
Geraniin	0.1	0.1	0.1	0.1	0.1	0.1
Squalene	0.7	0.7	0.7	-	-	-
Soy Phosphatidylcholine	4	4	4	4	4	4
Tween 80	0.7	-	-	0.7	-	-
Phosphate Buffer Saline	Up to 100	Up to 100	Up to 100	Up to 100	Up to 100	Up to 100

The thin film was left to settle overnight at room temperature. The next day, 100 mL of phosphate buffer solution (PBS) was introduced to hydrate the film overnight. On the

subsequent day, the mixture underwent homogenization using an Ultrasonicator operating at 50% power for 5 mins, with 1-minute intervals per cycle. To minimize the size of the GNP, extrusion was performed using an Avanti Mini Extruder (Avanti® Polar Lipids, United States). The resulting formulation was then divided into two portions: one stored at room temperature and the other at 4°C for stability testing.

TABLE II: Formulation compositions with and without geraniin.

Sample Name	SPC (4% w/v)	Tween 80 (0.7% w/v)	Squalene (0.7% w/v)	Geraniin (0.1% w/v)
ST - Blank	■	■		
STQ - Blank	■	■	■	
STG	■	■		■
STQG	■	■	■	■

2.2.2.1 Physicochemical characterisation of the geraniin nano-phytosomes (GNP)

Encapsulation efficiency (EE%)

The encapsulation efficiency (EE) percentages can be determined using the centrifugation method. The amount of free geraniin was quantified using a validated reversed-phase HPLC method (Agilent, California, USA) at 280nm, and calculated using the following equation:

$$EE = \frac{Qt - Qs}{Qt} \times 100 \qquad \textbf{(Equation 2)}$$

Where, EE is the entrapment efficiency, Q_t is the amount of geraniin added and Q_s is the amount of geraniin detected in the supernatant. The unentrapped geraniin in the dispersion was separated by the centrifugation method. 1 mL of sample was mixed with 1 mL of acetonitrile and centrifuged 10 min at 13,000 rpm for three times. 1 mL of supernatant was withdrawn and replaced with fresh acetonitrile after each centrifuge. The supernatant was pooled together and 1 mL of supernatant was filtered with a 45 µm syringe filter into an HPLC vial. The concentration of geranin in the supernatant was determined via HPLC in triplicates.

Particle diameter (Z-average), Polydispersity index (PDI) and Zeta potential of GNPs

The particle size, polydispersity index (PDI) and zeta potential of the GNP were determined at 25°C by dynamic light scattering (DLS) method (Zetasizer Nano-ZS installed with Zetasizer software (DTS v 6.12), Malvern Instruments, Malvern, UK). Samples were diluted with distilled water (1:10) before analysis. Measurements were taken in triplicates.

Morphological studies with Transmission Electron Microscopy (TEM)

The surface morphology of the prepared nano-phytosomes was visualized by transmission electron microscopy (TEM) (TECNAI G2 F20 X-Twin). The samples were placed on carbon-coated copper grids followed by negative staining using phosphotungstic acid (PTA) (2%) and viewed under the microscope with an accelerated 200kV [29].

Long-term stability studies of GNP formulations

The physical-chemical stability of the formulations was conducted at two different conditions: Refrigerated (4 ± 2°C) and Room temperature (25 ± 2°C). The entrapment efficiency, particle size of the formulations was evaluated once every month for three months.

2.2.2.2 Permeability studies of GNP via *in vitro* studies.

In vitro permeability studies of the optimized geraniin nano-phytosome formulation were conducted using a Strat-M® synthetic membrane on a Franz diffusion cell (EDC-07, Electrolab, India). The membrane was mounted between the donor and receiver compartments of the Franz diffusion cell, with a diffusion area of 1.77 cm^2. The receptor medium consisted of 5 mL of 0.2% (w/v) sodium lauryl sulfate (SLS) in phosphate-buffered saline (PBS) at pH 7.4, and was constantly stirred at 100 rpm with a small magnetic bar. The receptor compartment was maintained at a temperature of 37 ± 0.2°C using a circulating water jacket. 1 mL of the developed formulation was placed in the donor compartment for the permeability study.

Sample collection from receptor chamber

Samples of 0.5 mL were withdrawn from the receptor compartment via the sampling port at specified time intervals (0, 0.5, 1, 1.5, 2, 4, 6, 8, 22, and 24 hours) and immediately replaced with an equal volume of fresh receptor solution to maintain sink conditions. Triplicate experiments were conducted for each study. The collected samples were analyzed for geraniin content using HPLC.

Membrane extraction

After the 24-hour permeability study, the membrane was collected to determine the amount of geraniin accumulated within it. The membrane was cut into smaller pieces and placed in a beaker. A mixture of 1 mL acetonitrile and 1 mL phosphate buffer solution with 0.2% SLS was added to the beaker. The beaker was incubated and shaken at 100 rpm at room temperature for 24 hours to facilitate membrane extraction. The geraniin content in the collected samples was analyzed via HPLC.

3.0 Results

3.1 Skin aging inhibitory action assay

Skin aging is known to result in the decrease of the amount of elastin and collagen presented in the dermal layer of human skin, resulting in the loss of strength and flexibility in the skin. The anti-aging properties of the extracts were assessed by measuring their ability to inhibit elastase and collagenase activity. The AGE inhibitory, collagenase and elastase inhibition effects of tested samples (pure Geraniin, crude extracts, squalene and ellagic acid) at a final concentration of 1 mg/ml were determined and elucidated as shown in **Figure 1 (a, b and c)**. In our investigation, we found positive influences of Geraniin, the crude extract, squalene and ellagic acid on the inhibition of AGE, as monitored by the BSA-MGO system **(Figure 1 (a))**. The positive control, aminoguanidine (AG), highly inhibited formation of fluorescent AGEs (96.31 ± 0.05%). Geraniin (26.44 ± 1.23 %), the crude extract (17.81 ± 2.86 %), and ellagic acid (38.92 ± 1.15 %), whereas squalene possesses the lowest ability to inhibit AGE formation. The rank of AGE inhibition ability was as follows: Ellagic Acid > Geraniin > crude extract > squalene. The collagenase inhibitory activity of Geraniin (102.31 ± 3.40%) and the crude ethanolic extract (83.04 ± 8.44 %) was comparable with the positive control, 1,10-Phenanthroline (92.90 ± 7.8 %) **(Figure 1 (b))**. However, squalene and Ellagic acid, the metabolite of geraniin, showed no significant inhibition in comparison to the positive control

(p<0.001). Reduction in elastase activity up to 40% has been observed by crude extract and ellagic acid. However, this is in contrast to the increase in elastase activity of the positive control, MAAPV (72.57 ± 0.15 %). Interestingly, Geraniin showed 19.46 ± 1.25 % inhibition, while squalene exhibited no inhibitory activity. Comparing the three mechanistic studies on skin anti-aging, collagenase inhibitory activity of Geraniin was the strongest, while elastase activity can be considered as moderate and AGE inhibitory activity as weak.

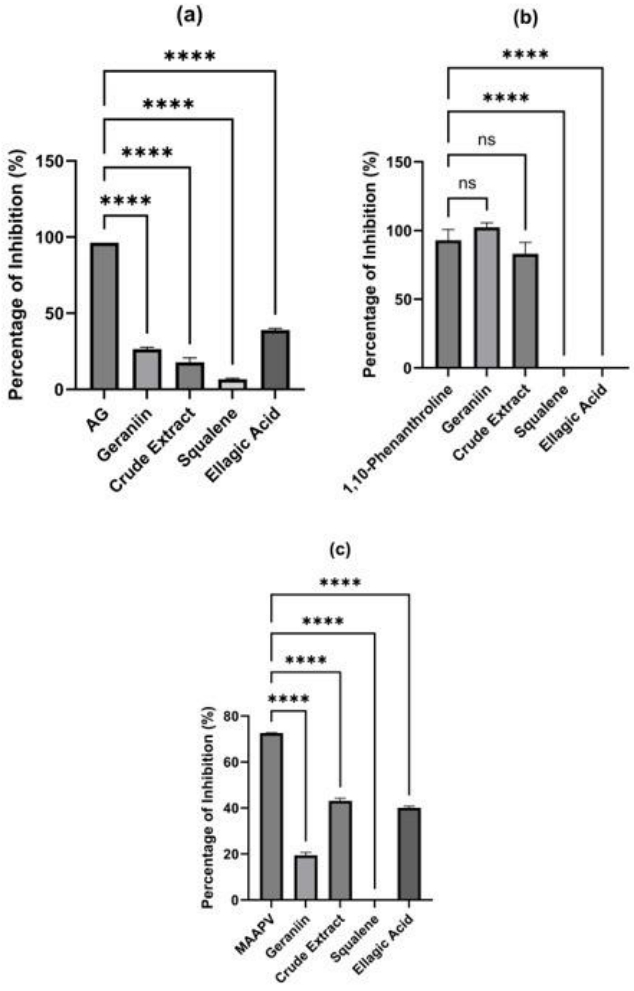

Figure 1: The ability of Geraniin, crude extract, ellagic acid and squalene to inhibit AGEs formation measured in (a) BSA-MGO model systems; (b) Collagenase inhibition and (c) elastase. AG: aminoguanidine; AGEs:

Advanced Glycation End- products; MAAPV - N-Methoxysuccinyl-Ala-Ala-Pro-Val-chloromethyl ketone. (******** *p<0.001*)

3.2 Development of Geraniin (GE) nano-phytosome (GNP)

Following a thorough preliminary study, the GNP formulation using Tween 80 as the edge activator, with the combination of dichloromethane and ethanol as solvents and squalene as a preservative demonstrated promising results without any observable separation.

3.2.1 Physicochemical characterisation of the geraniin nano-phytosomes (GNP)

3.1.1 Encapsulation efficiency (EE%)

Based on the results described in **Figure 2**, we noted a significant difference in the EE% between the STG (63.74 ± 1.18 %) and STQG formulations (67.61 ± 2.06 %) (*p* <0.05).

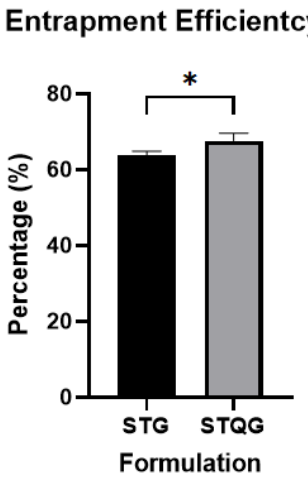

Figure 2: Mean value of entrapment efficiency (Mean ± S.D). (Note: * indicates the significant values of (*p*<0.05) between the respective formulations (STG and STQG)).

3.1.2 Particle diameter (Z-average), Polydispersity index (PDI) and zeta potential of GNPs

A significant difference in the particle size and polydispersity index were identified between STG and STQG formulations (p<0.0001) **(TABLE III)**. There was no significance in particle size and polydispersity index between STG and ST. However, it was interesting to note that there was a significance difference in particle size between STQ and STQG, (p< 0.0001) while particle size difference between ST and STG were non-significant. Conversely, no significant differences in PDI were noted between the ST and STG formulations, nor between the STQ and STQG formulations.

The zeta potential measurements for the nano-phytosome formulations reveal significant differences in colloidal stability based on the composition of the formulations. As shown in **TABLE III**, the zeta potential values demonstrate that the addition of squalene and geraniin to the phospholipid and Tween 80 base significantly enhances the stability of nano-phytosome formulations (p<0.0001). The STQG formulation, with the highest zeta potential magnitude of -17.0 mV, shows the greatest stability, making it the most suitable for applications ensuring prolonged stability and minimal aggregation.

TABLE III: The particle size, polydispersity index (PDI), and zeta potential of four nanophytosome formulations: with geraniin (STG), without geraniin (ST), with squalene (STQ), and without squalene (STQG).

Sample Name	**Z-Average (d.nm)** **(Mean ± S.D)**	**Polydispersity index (PDI)** **(Mean ± S.D)**	**Zeta potential (mV)** **(Mean ± S.D)**
(ST) - Blank	61.04 ± 0.274	0.263 ± 0.003	-5.5 ± 0.73
(STQ) - Blank	88.72 ± 0.150	0.154 ± 0.009	-9.17 ± 0.82
(STG)	60.29 ± 0.482	0.244 ± 0.002	-11.47 ± 0.25

(STQG)	95.60 ± 0.460	0.167 ± 0.014	-17.0 ± 1.70

3.1.3 Morphological studies with Transmission Electron Microscopy (TEM)

The structure and morphology of the vesicles were analyzed using Transmission Electron Microscopy (TEM). TEM images demonstrated that the nano-phytosomes displayed spherical and oval shapes with unilamellar structures, confirming their composition of a single lipid bilayer and indicating successful formation of nano-phytosomal vesicles **(Figure 3)**.

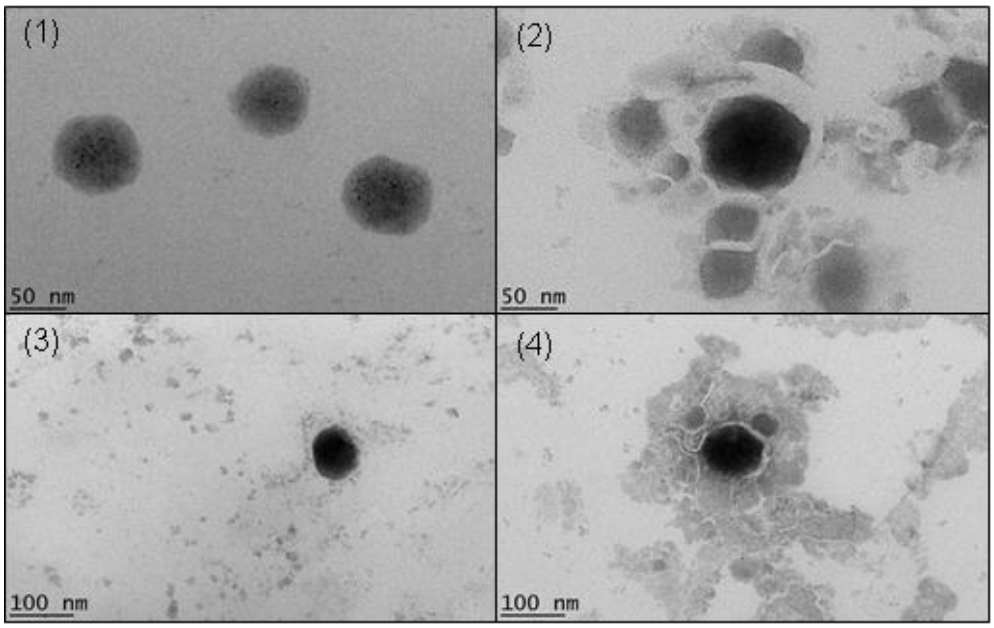

Figure 3: Surface morphology of nanophytosomes by transmission electron microscopy (TEM) (Note: 1:ST; 2: STQ; 3: STG; 4: STQG).

3.1.4 Long-term stability studies of GNP formulations

Stability is a crucial factor in ensuring the safety and efficacy of drug products, and it is an obligatory step in the development process. The stability of the GNP was observed for a period of 3 months evaluated under two distinct storage conditions: 25°C ± 2°C (room temperature) and 4°C ± 3°C (refrigerated). These stability studies included the monitoring of any alterations in the physical appearance and drug leakage of the complex. The entrapment efficiency (**Figure 4**) and particle size analysis (**Figure 5**) of the GNP remained consistently stable when stored under refrigerated conditions for 90 days, showing no significant differences. This highlights its robust stability and resistance to degradation during refrigerated storage. In contrast, formulations stored at room temperature exhibited a notable increase in both entrapment efficiency and particle size over the same period ($p < 0.0001$).

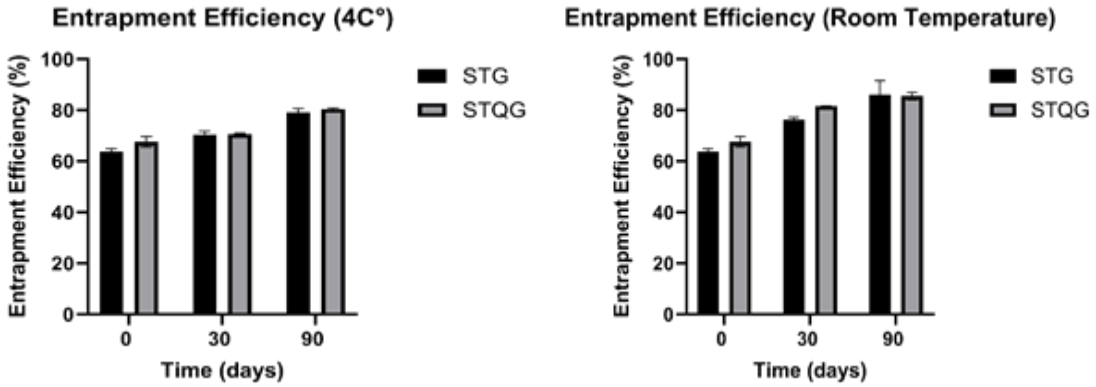

Figure 4: Long-Term Stability of Nanophytosomes: Entrapment Efficiency Over 90 Days.

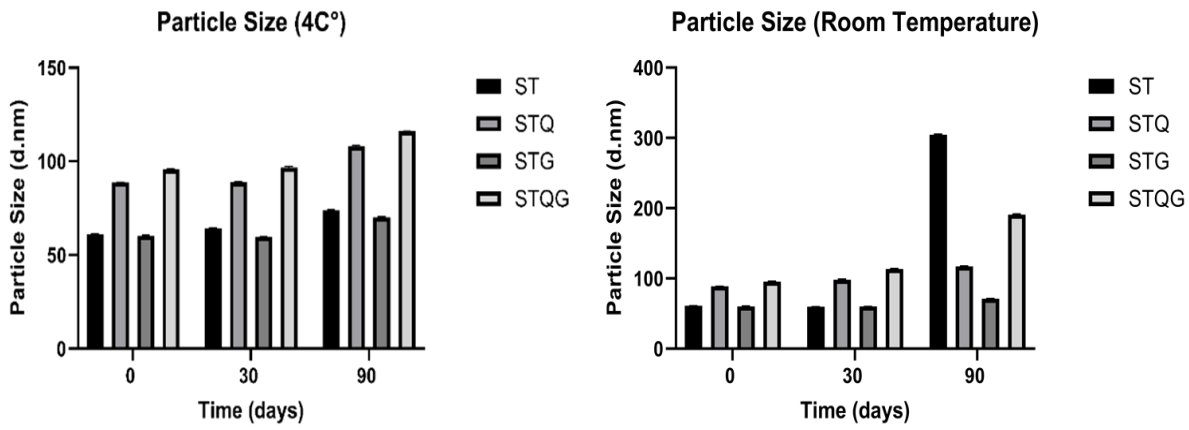

Figure 5: Long-term stability of nanophytosomes: Particle size analysis over 90 days

3.4.3 Permeability studies of GNP via *in vitro* studies.

Permeability studies of GNP using Franz diffusion cell indicated that no geraniin was detected in the receptor chamber sample, suggesting that the GNP is not suitable for transdermal application. However, upon digestion and extraction of the membrane, significant accumulation of geraniin was observed in formulations containing squalene (STQG) compared to the formulation without squalene (STQ) ($p \leq 0.0001$) (**Figure 6**). This confirms that the GNP is more effective as a topical formulation, particularly when formulated with squalene (STQG).

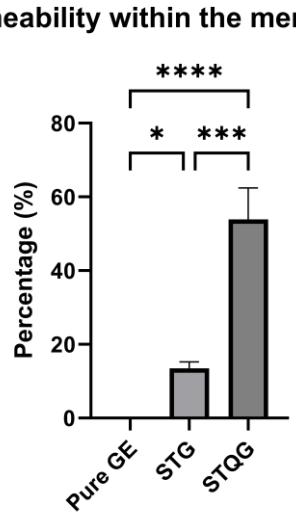

Figure 6: Accumulation of Geraniin within the membrane (%) (Mean ± S.D) (ANOVA). (Note: * indicates the significant values of ($p < 0.05$); *** indicates significant values of ($p \leq 0.0002$); **** indicates significant values of ($p < 0.0001$), between the respective formulations (Pure GE, STG, and STQG)).

Discussion.

Collagen plays an important role in the elasticity of skin connective tissues with diversified structures. Collagenolytic MMP enzymes attack fibrillar collagen and elastin responsible for the dermal strength and resiliency [30]. It is deemed that the MMP inhibition is one of the strategies to prevent UV-triggered photodamage. Geraniin emerges as a promising candidate for anti-aging skincare formulations due to its notable collagenase inhibitory activity and moderate elastase inhibition. AGEs, formed when sugars react with proteins, lipids, or nucleic acids, speed up skin aging. Methylglyoxal (MGO), a key intermediate, worsens this by linking collagen and elastin fibers, decreasing skin elasticity and causing wrinkles. AGEs also provoke inflammation and oxidative stress, harming skin cells and structure. They hinder cellular functions and repair processes, accelerating skin aging, especially through MGO accumulation [31]. Geraniin's ability to inhibit AGE formation also suggests potential benefits in preventing glycation-related skin aging processes. In contrast, while squalene is valued for its skin

penetration enhancement properties, it did not show significant anti-aging enzymatic inhibition in this study. Further research could explore synergistic effects of combining Geraniin with squalene or other compounds to enhance overall anti-aging efficacy in skincare applications.

This study utilized geraniin extracted from rambutan rind, known for its potent antioxidant properties surpassing those of vitamin C. Despite its high molecular weight hindering skin absorption, nano-phytosome technology was employed to enhance the delivery and bioavailability of Geraniin [22, 32]. Nano-phytosome, a lipid-based drug delivery mechanism embeds phytoconstituents into the head of a phospholipid such as phosphatidylcholine [33].

The study's investigation of the GNP builds on preliminary studies and recent publications that utilized Tween 80 in nano-phytosome formulations [34]. In addition, squalene (STGaia™), a natural plant squalene with tocotrienols/tocopherols, naturally extracted from palm fruits was added into the formulation as a preservative. Squalene, a triterpene found in various oils and human sebum, is valued for its antioxidant and skin hydration properties. It enhances skin condition by promoting collagen production and improving the stability and permeation of topical formulations [35, 36].

The significantly higher EE % (**Figure 2**) and particle size (**TABLE III**) of STQG compared to STG could be attributed to the presence of squalene as an excipient in the STQG formulation. Similar study has demonstrated squalene to enhance the entrapment efficiency by providing a more flexible and accommodating lipid environment for the encapsulation of active compounds like Geraniin [37]. Its hydrophobic nature helps stabilize hydrophobic interactions with Geraniin molecules, leading to better encapsulation within the lipid bilayer of the nano-phytosome. Additionally, the inclusion of squalene can increase particle size due to its bulky structure and ability to influence the packing of lipid bilayers. Squalene's integration into the nano-phytosome structure may cause the lipid bilayers to adopt a more expanded conformation, resulting in larger vesicles. Nevertheless, the lower PDI values obtained depicted a more monodisperse

formulation that was less susceptible to aggregation. Moreover, zeta potential, a valuable indicator of physical stability and effective distribution of colloidal particles in an aqueous medium, demonstrated that STQG is the most stable formulation compared to the others tested (**TABLE III**). This finding is supported by the nano-sized and unilamellar surface morphology observed in the optimized formulation (**Figure 3**). The long-term stability studies revealed that the encapsulation efficiency (EE%), particle size, and PDI of the GNP formulation showed superior results when stored at 4°C compared to 25°C **(Figure 4 & 5)**. However, the necessity for refrigerated storage poses a practical limitation for real-world application.

Assessing *in vitro* skin permeation is essential for comprehending the efficacy and safety of topically applied compounds. The dermal delivery of GNP was evaluated using STRAT-M® membranes, selected for their similarity to human skin. These membranes consist of multiple layers of polyether sulfone that offer penetration resistance, mimicking the skin's physiological barrier, with a single layer of polyolefin. This makes STRAT-M® membranes a suitable model for assessing dermal delivery efficacy [38]. The study results indicated that there was no permeation of geraniin across the membrane over 24 hours, suggesting that GNPs are not suitable for transdermal application. Due to its highly hydrophobic nature (log P = 12.86), squalene, when mixed with polyphenols, could potentially enhance the hydrophobic environment within the skin layers. This condition may lead to limited release of compounds into the receptor chamber, which consists of a highly hydrophilic medium (PBS, pH 7.4) [39]. On the contrary, a significant increase in Geraniin accumulation within the membranes treated with squalene-containing formulations (STQG) compared to those without squalene (STQ) ($p \leq 0.0001$) (**Figure 6**) was observed. This confirms the efficacy of GNPs as a topical formulation, particularly in combination with squalene. Previous research has demonstrated squalene's capability to penetrate human skin effectively and improve the transport and absorption of other active ingredients [40]. This study highlights squalene's potential as a skin penetration enhancer for polyphenols, which enhances their longevity in the skin. This ability of squalene to

prolong dermal exposure to polyphenols is particularly beneficial for developing products focused on anti-aging benefits.

Conclusion.

This study underscores geraniin's potential as a potent anti-aging agent, particularly when formulated into nano-phytosomes. Geraniin exhibited significant collagenase inhibitory activity, moderate elastase inhibition, and the ability to reduce advanced glycation end-product (AGE) formation. Incorporating squalene into the formulation notably enhanced geraniin's penetration and retention in the skin, prolonging its effectiveness. While squalene itself did not exhibit substantial anti-aging enzymatic inhibition, its role as a skin penetration enhancer is crucial for enhancing the efficacy of topical formulations containing polyphenols like geraniin. These findings highlight the promise of combining natural compounds with advanced delivery systems to create highly effective anti-aging skincare products. Future research should explore synergistic effects between geraniin and other compounds to optimize their anti-aging benefits further.

Acknowledgments.

The authors would like to acknowledge the Ministry of Higher Education (MOHE) for funding under the Fundamental Research Grant Scheme (FRGS) (FRGS/1/2020/SKK06/MUSM/03/2).

Conflict of Interest Statement.

The authors declare that they have no known competing financial interests or personal relationships that could have appeared to influence the work reported in this paper.

References.

1. Gu, Y., J. Han, C. Jiang, and Y. Zhang, *Biomarkers, oxidative stress and autophagy in skin aging.* Ageing Research Reviews, 2020. **59**: p. 101036.
2. Gruber, F., C. Kremslehner, L. Eckhart, and E. Tschachler, *Cell aging and cellular senescence in skin aging — Recent advances in fibroblast and keratinocyte biology.* Experimental Gerontology, 2020. **130**: p. 110780.
3. Shin, S.H., Y.H. Lee, N.K. Rho, and K.Y. Park, *Skin aging from mechanisms to interventions: focusing on dermal aging.* Front Physiol, 2023. **14**: p. 1195272.
4. Slominski, A. and J. Wortsman, *Neuroendocrinology of the skin.* Endocr Rev, 2000. **21**(5): p. 457-87.
5. Wong, Q.Y.A. and F.T. Chew, *Defining skin aging and its risk factors: a systematic review and meta-analysis.* Sci Rep, 2021. **11**(1): p. 22075.
6. Aguilar-Toalá, J.E., A. Vidal-Limon, and A.M. Liceaga, *Chapter Six - Nutricosmetics: A new frontier in bioactive peptides' research toward skin aging*, in *Advances in Food and Nutrition Research*, F. Toldrá, Editor. 2023, Academic Press. p. 205-228.
7. Sreedhar, A., L. Aguilera-Aguirre, and K.K. Singh, *Mitochondria in skin health, aging, and disease.* Cell Death & Disease, 2020. **11**(6): p. 444.
8. He, X., F. Wan, W. Su, and W. Xie, *Research Progress on Skin Aging and Active Ingredients.* Molecules, 2023. **28**(14): p. 5556.
9. Ndlovu, G., et al., *In vitro determination of the anti-aging potential of four southern African medicinal plants.* BMC Complementary and Alternative Medicine, 2013. **13**(1): p. 304.

10. Shin, J.W., et al., *Molecular Mechanisms of Dermal Aging and Antiaging Approaches.* Int J Mol Sci, 2019. **20**(9).

11. Dhalaria, R., et al., *Bioactive Compounds of Edible Fruits with Their Anti-Aging Properties: A Comprehensive Review to Prolong Human Life.* Antioxidants, 2020. **9**(11): p. 1123.

12. Pan, S.-Y., et al., *Historical Perspective of Traditional Indigenous Medical Practices: The Current Renaissance and Conservation of Herbal Resources.* Evidence-based complementary and alternative medicine : eCAM, 2014. **2014**: p. 525340.

13. Ganesan, P. and D.K. Choi, *Current application of phytocompound-based nanocosmeceuticals for beauty and skin therapy.* Int J Nanomedicine, 2016. **11**: p. 1987-2007.

14. Cruz, A.M., et al., *In Vitro Models for Anti-Aging Efficacy Assessment: A Critical Update in Dermocosmetic Research.* Cosmetics, 2023. **10**(2): p. 66.

15. Alvarado-Morales, G., et al., *Application of thermosonication for Aloe vera (Aloe barbadensis Miller) juice processing: Impact on the functional properties and the main bioactive polysaccharides.* Ultrasonics Sonochemistry, 2019. **56**: p. 125-133.

16. Huyop, F., et al., *Physicochemical and antioxidant properties of Apis cerana honey from Lombok and Bali Islands.* Plos one, 2024. **19**(4): p. e0301213.

17. Henning, S.M., et al., *Pomegranate Juice and Extract Consumption Increases the Resistance to UVB-induced Erythema and Changes the Skin Microbiome in Healthy Women: a Randomized Controlled Trial.* Sci Rep, 2019. **9**(1): p. 14528.

18. Kang, S.J., et al., *Beneficial effects of dried pomegranate juice concentrated powder on ultraviolet B-induced skin photoaging in hairless mice.* Exp Ther Med, 2017. **14**(2): p. 1023-1036.

19. Elendran, S., S. Muniyandy, W. Lee, and U. Palanisamy, *Permeability of the ellagitannin geraniin and its metabolites in a human colon adenocarcinoma Caco-2 cell culture model.* Food & Function, 2018. **10**.

20. Boonpisuttinant, K., et al., *In vitro anti-ageing activities of ethanolic extracts from Pink rambutan (Nephelium lappaceum Linn.) for skin applications.* Saudi Pharm J, 2023. **31**(4): p. 535-546.

21. Thitilertdecha, N., P. Chaiwut, and N. Saewan, *In vitro antioxidant potential of Nephelium lappaceum L. rind extracts and geraniin on human epidermal keratinocytes.* Biocatalysis and Agricultural Biotechnology, 2020. **23**: p. 101482.

22. Elendran, S., L. Wang, R. Prankerd, and U. Palanisamy, *The physicochemical properties of geraniin, a potential antihyperglycemic agent.* Pharmaceutical biology, 2015. **53**: p. 1-8.

23. Dewi, M.K., A.Y. Chaerunisaa, M. Muhaimin, and I.M. Joni, *Improved Activity of Herbal Medicines through Nanotechnology.* Nanomaterials (Basel), 2022. **12**(22).

24. Rohman, A., *Physico-chemical Properties and Biological Activities of Rambutan (Nephelium lappaceum L.) Fruit.* Research Journal of Phytochemistry, 2017. **11**: p. 66-73.

25. Starowicz, M. and H. Zieliński, *Inhibition of Advanced Glycation End-Product Formation by High Antioxidant-Leveled Spices Commonly Used in European Cuisine.* Antioxidants (Basel), 2019. **8**(4).

26. Quinty, V., et al., *Screening and Evaluation of Dermo-Cosmetic Activities of the Invasive Plant Species Polygonum cuspidatum.* Plants, 2023. **12**(1): p. 83.

27. Eun, C.-H., M.-S. Kang, and I.-J. Kim, *Elastase/Collagenase Inhibition Compositions of Citrus unshiu and Its Association with Phenolic Content and Anti-Oxidant Activity.* Applied Sciences, 2020. **10**(14): p. 4838.

28. Moorthy, M., J.J. Khoo, and U.D. Palanisamy, *Acute oral toxicity of the ellagitannin geraniin and a geraniin-enriched extract from Nephelium lappaceum L rind in Sprague Dawley rats.* Heliyon, 2019. **5**(8): p. e02333.

29. Salem, H.F., et al., *Mitigation of Rheumatic Arthritis in a Rat Model via Transdermal Delivery of Dapoxetine HCl Amalgamated as a Nanoplatform: In vitro and in vivo Assessment.* International Journal of Nanomedicine, 2020. **15**(null): p. 1517-1535.

30. Tzaphlidou, M., *The role of collagen and elastin in aged skin: an image processing approach.* Micron, 2004. **35**(3): p. 173-177.

31. Chen, C.-y., et al., *Advanced Glycation End Products in the Skin: Molecular Mechanisms, Methods of Measurement, and Inhibitory Pathways.* Frontiers in Medicine, 2022. **9**.

32. Cheng, H.S., S. Ton, and K. Kadir, *Ellagitannin geraniin: a review of the natural sources, biosynthesis, pharmacokinetics and biological effects.* Phytochemistry Reviews, 2017. **16**.

33. Gaikwad, S.S., et al., *Overview of phytosomes in treating cancer: Advancement, challenges, and future outlook.* Heliyon, 2023. **9**(6): p. e16561.

34. Baradaran, S., A. Hajizadeh Moghaddam, S. Khanjani Jelodar, and N. Moradi-Kor, *Protective Effects of Curcumin and its Nano-Phytosome on Carrageenan-Induced Inflammation in Mice Model: Behavioral and Biochemical Responses.* J Inflamm Res, 2020. **13**: p. 45-51.

35. Dutta, M., S. Sarkar, P. Karmakar, and S. Mandal Biswas, *A squalene analog 4,4'-diapophytofluene from coconut leaves having antioxidant and anti-senescence potentialities toward human fibroblasts and keratinocytes.* Scientific Reports, 2024. **14**(1): p. 12593.

36. Gref, R., et al., *Vitamin C-squalene bioconjugate promotes epidermal thickening and collagen production in human skin.* Sci Rep, 2020. **10**(1): p. 16883.

37. Arias, J.L., et al., *Squalene based nanocomposites: a new platform for the design of multifunctional pharmaceutical theragnostics.* ACS Nano, 2011. **5**(2): p. 1513-21.

38. Uchida, T., et al., *Prediction of skin permeation by chemical compounds using the artificial membrane, Strat-M (TM).* European journal of pharmaceutical sciences : official journal of the European Federation for Pharmaceutical Sciences, 2014. **67C**: p. 113-118.

39. Moldoveanu, S. and V. David, *Chapter 6 - Solvent Extraction*, in *Modern Sample Preparation for Chromatography*, S. Moldoveanu and V. David, Editors. 2015, Elsevier: Amsterdam. p. 131-189.

40. Oliveira, A.L.S., et al., *Effect of squalane-based emulsion on polyphenols skin penetration: Ex vivo skin study.* Colloids and Surfaces B: Biointerfaces, 2022. **218**: p. 112779.